# Fourier transform infrared (FTIR) spectroscopy

**Article** *in* Photosynthesis Research · July 2009

DOI: 10.1007/s11120-009-9439-x · Source: PubMed



**2 authors**, including:

Catherine Berthomieu
Atomic Energy and Alternative Energies Commission
**99** PUBLICATIONS **2,348** CITATIONS

SEE PROFILE

Photosynth Res (2009) 101:157–170
DOI 10.1007/s11120-009-9439-x

REVIEW

# Fourier transform infrared (FTIR) spectroscopy

**Catherine Berthomieu · Rainer Hienerwadel**

Received: 18 February 2009 / Accepted: 15 May 2009 / Published online: 10 June 2009


**Abstract** Fourier transform infrared (FTIR) spectroscopy probes the vibrational properties of amino acids and cofactors, which are sensitive to minute structural changes. The lack of specificity of this technique, on the one hand, permits us to probe directly the vibrational properties of almost all the cofactors, amino acid side chains, and of water molecules. On the other hand, we can use reaction-induced FTIR difference spectroscopy to select vibrations corresponding to single chemical groups involved in a specific reaction. Various strategies are used to identify the IR signatures of each residue of interest in the resulting reaction-induced FTIR difference spectra. (Specific) Isotope labeling, site-directed mutagenesis, hydrogen/deuterium exchange are often used to identify the chemical groups. Studies on model compounds and the increasing use of theoretical chemistry for normal modes calculations allow us to interpret the IR frequencies in terms of specific structural characteristics of the chemical group or molecule of interest. This review presents basics of FTIR spectroscopy technique and provides specific important structural and functional information obtained from the analysis of the data from the photosystems, using this method.

**Keywords** Fourier transform infrared spectroscopy · Isotope-edited infrared spectroscopy · Metal–ligands · Water molecules

Special Issue of Photosynthesis Research "Basics and Applications of BiophysicalTechniques in Photosynthesis and Related Processes", edited by Messinger, Alia and Govindjee.

C. Berthomieu (✉)
CEA (Commissariat à l' Energie Atomique), Laboratoire des Interactions Protéine Métal, DSV (Direction des Sciences du Vivant), Institut de Biologie Environnementale et Biotechnologie, Service de Biologie Végétale et Microbiologie Environnementales (DSV/iBEB/SBVME), CEA-Cadarache, UMR 6191 Centre National de la Recherche Scientifique (CNRS)-CEA (Commissariat à l' Energie Atomique)-Université Aix-Marseille II, 13108 Saint Paul-lez-Durance Cedex, France
e-mail: catherine.berthomieu@cea.fr

R. Hienerwadel
Aix-Marseille Université, Laboratoire de Génétique et de Biophysique des Plantes, Faculté des Sciences de Luminy, Direction des Sciences du Vivant, Institut de Biologie Environnementale et Biotechnologie, Service de Biologie Végétale et Microbiologie Environnementales (DSV/iBEB/SBVME), UMR 6191 Centre National de la Recherche Scientifique (CNRS)-CEA (Commissariat à l' Energie Atomique)-Université Aix-Marseille II, 13288 Marseille cedex 9, France

## List of abbreviations

| | |
|---|---|
| ATR | Attenuated total reflection |
| BChl | Bacteriochlorophyll |
| CVD | Chemical vapor deposition |
| ENDOR | Electron nuclear double resonance |
| ESEEM | Electron spin echo envelope modulation |
| FTIR | Fourier transform infrared |
| IR | Infrared |
| $P_{700}$ | Primary electron donor of PSI |
| PSI | Photosystem I |
| PSII | Photosystem II |
| $Q_A$, $Q_B$ | Primary and secondary electron acceptor quinones of photosynthetic RCs |
| RC | Reaction center |
| $Tyr_D$, $Tyr_Z$ | The two redox active tyrosines of PSII |
| WT | Wild type |

## Introduction

Infrared (IR) or Fourier transform infrared (FTIR) spectroscopy has a large application range, from the analysis of

small molecules or molecular complexes to the analysis of cells or tissues. The imaging of tissues is one of the recent developments of infrared spectroscopy, taking advantage of infrared microscopy and of the use of synchrotron IR radiation. It is used for the mapping of cellular components (carbohydrates, lipids, proteins) to identify abnormal cells (Levin and Bhargava 2005; Petibois and Déléris 2006). FTIR spectroscopy has also been increasingly applied to the study of proteins. This concerns the analysis of protein conformation, protein folding, and of molecular details from protein active sites during enzyme reactions using reaction-induced FTIR difference spectroscopy (Siebert and Hildebrandt 2008).

FTIR difference spectroscopy has been widely applied in photosynthesis research and related areas. This approach gives complementary information to the three-dimensional structural data obtained by X-ray diffraction (or Nuclear Magnetic Resonance, NMR). The analysis of active sites in proteins by means of reaction-induced FTIR difference spectroscopy gives information on minute structural changes, hydrogen-bonding interactions, and proton transfer reactions, which are often beyond the sensitivity of X-ray diffraction analyses. Moreover, time-resolved techniques, with time resolution now up to the femtosecond range (Di Donato et al. 2008) allow structural changes to be observed for protein active sites "at work".

In photosynthesis, this approach has given information of prime interest concerning the cofactor-protein interactions (Nabedryk 1996; Breton 2001; Berthomieu and Hienerwadel 2005; Noguchi and Berthomieu 2005), as well as proton transfer routes in bacterial reaction centers (Nabedryk and Breton 2008). It now plays a central role in the detailed analysis of the oxygen evolving complex of Photosystem II (Chu et al. 2001; Noguchi 2007; Debus 2008).

While this approach suffers from several limitations, it delivers unique information by addressing directly the properties of cofactors, amino acids, and water molecules, with very high sensitivity to structural parameters and electronic interactions. This justifies the experimental efforts that have been made to optimize its use and the interpretation of the data.

In the following, we briefly present the principles of infrared spectroscopy and describe the development of experimental approaches to identify and analyze IR signatures from active sites in proteins by reaction-induced FTIR difference spectroscopy. We describe the methodology to obtain reliable spectra and interpretations, and show typical examples of specific information brought by this technique in the study of photosystems.[1]

[1] We do not present an exhaustive review of the FTIR literature on photosystems.

## Principle and methodology of infrared spectroscopy and FTIR difference spectroscopy

### Infrared spectroscopy

Infrared spectroscopy probes the molecular vibrations. Functional groups can be associated with characteristic infrared absorption bands, which correspond to the fundamental vibrations of the functional groups (Colthup et al. 1975; Griffith and de Haseth 1986). For a nonlinear molecule with N atoms, there are 3N-6 vibrational motions of the molecule atoms, or 3N-6 fundamental vibrations or normal modes. A normal mode of vibration is infrared active (i.e., it absorbs the incident infrared light) if there is a change in the dipole moment[2] of the molecule during the course of the vibration. Thus, symmetric vibrations are usually not detected in infrared. In particular, when a molecule has a center of symmetry, all vibrations which are symmetrical with respect to the center are infrared inactive. In contrast, the asymmetric vibrations of all molecules are detected. This lack of selectivity allows us to probe the properties of almost all chemical groups in one sample, and notably of amino acids and water molecules which can hardly be observed by other spectroscopic techniques.

Strong IR absorptions are observed for groups with a permanent dipole (i.e., for polar bonds). As such, the carbonyl groups of the polypeptide backbone contribute largely to the infrared absorption spectra of proteins.

In the mid-infrared region (4,000–1,000 $cm^{-1}$), two main types of vibrations are observed: vibrations along chemical bonds, called stretching vibrations ($\nu$), which involve bond-length changes; and vibrations involving changes in bond angles, and notably bending vibrations ($\delta$—in plane, $\pi$—out of plane).

The stretching vibrations can be modeled using the harmonic oscillator model (Fig. 1), in which a chemical bond is represented by two point masses linked by a spring. The bond strength (or molecular force field) is the spring tenseness $k$ and the point masses ($m_1$ and $m_2$) model the masses of the atoms or chemical groups involved in the bond. The oscillation frequency $\nu$ is given by the equation[3]:

$$\nu = (1/2\pi c)\sqrt{(k(m_1 + m_2)/m_1 m_2)}.$$

The vibration frequency $\nu$ thus depends on the bond strength, with higher frequencies for triple or double bonds as compared to single bonds. This is illustrated in Fig. 1 for CO bonds. A consequence of the dependence of stretching mode frequencies on the bond strength is that the

[2] Dipole moment: when a positive charge $+z$ and a negative charge $-z$ are separated by a distance $d$, the dipole moment $\mu$ is equal to the magnitude of the charge multiplied by the distance ($\mu = zd$). .

[3] In the FTIR spectra, the infrared absorption is given as a function of the vibration frequency expressed in $cm^{-1}$.

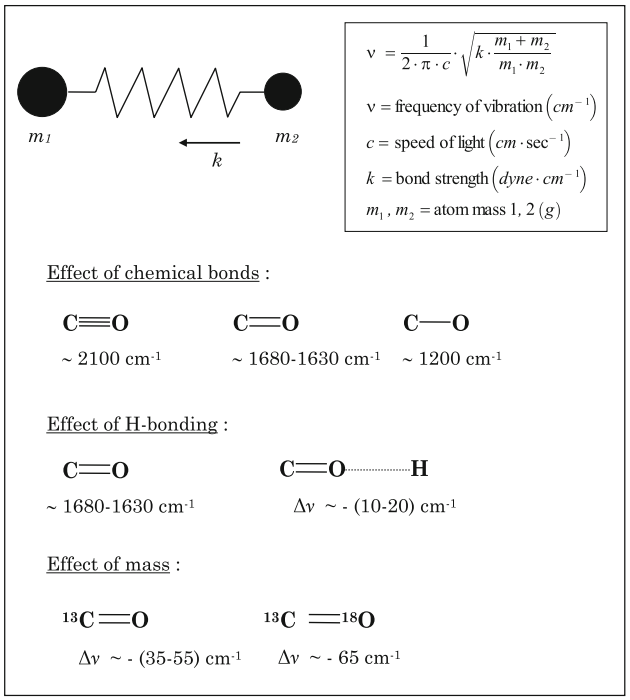


**Fig. 1** Stretching vibrations can be approximately determined using the harmonic oscillator model. The infrared absorption frequencies, $\nu$, of these vibrations depend on the nature of the chemical bonds, interactions with the environment (e.g., H-bonding) and relative masses of the atoms involved in the vibration. Typical frequency-shifts are indicated for $\nu$(CO) vibrations for these effects

frequencies are very sensitive to the group environment, the electronegativity of neighboring atoms or groups, or to hydrogen bonding interactions. The involvement of one of the atoms in a hydrogen bond will induce a weakening of the bond strength, and thus a frequency downshift of the stretching mode of the chemical group (Fig. 1). The sensitivity of this method is high, and corresponds to changes in bond length smaller than 0.2 Å (Deng and Callender 1999; Barth 2007). For a carbonyl group, formation of a hydrogen bond induces downshifts up to 20 $cm^{-1}$. The inspection of stretching mode frequencies of chemical groups, and specifically of carbonyl or carboxylic groups in proteins, reveals information on fine structural details. Formation or disruption of hydrogen bonding interactions is one of those.

The vibration frequency $\nu$ also depends on the mass of the atoms involved in the vibration. This effect is illustrated in Fig. 1. Consequently, it is possible to specifically alter a vibration frequency by isotope labeling of one of the atoms involved in the vibration. Substitution of hydrogen by deuterium has been widely used to identify and analyse groups with exchangeable protons. Specific isotope labeling ($^{13}C$, $^{15}N$, $^{18}O$, $^{2}H$) is also a very powerful approach to identify the frequency of one specific group in a complex infrared spectrum (see below).

In summary, the vibrational frequencies of a given chemical group are expected in specific regions which depend on the type of atoms involved and the type of chemical bonds. Tables are available for the main chemical groups, as well as for amino acid side chains (Venyaminov and Kalnin 1990a; Socrates 1994; Barth 2000; Wolpert and Hellwig 2006). Within these vibration regions, the frequencies of the chemical groups are modulated by the specific environment of the group. Therefore, to establish a clear relationship between the infrared mode frequency and the structural properties of a given residue, or when there are no data available in the tables, it is necessary to perform a detailed IR analysis on simplified model compounds in different environments (solvents) and/or to analyze experimental results using theoretical chemistry approaches.

*Absorption of proteins in solution*

The infrared absorption spectrum of proteins is dominated by the absorption of the peptide bonds (Fig. 2a). The $\nu$(C=O) modes of the peptide backbone contribute in the 1,680–1,620 $cm^{-1}$ range and form the Amide I band, while the peptide $\nu$(CN) + $\delta$(NH) modes contribute in the 1,560–1,520 $cm^{-1}$ range and form the Amide II band. The Amide I band of a protein depends on the tertiary structure of the protein, with distinct $\nu$(C=O) mode frequencies for $\alpha$-helices, turns, or $\beta$-sheet structures (Krimm and Bandekar

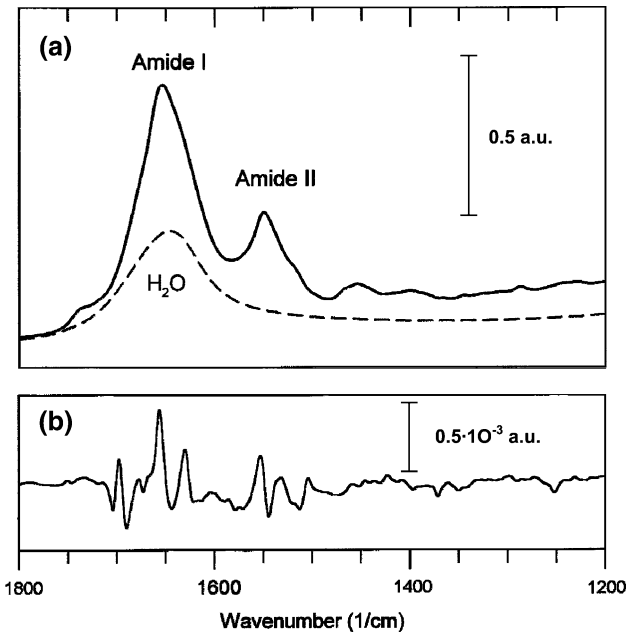


**Fig. 2 a** Infrared absorption spectrum of thylakoid membranes enriched in Photosystem II in the mid-infrared region (continuous line), contribution from water molecules of the buffer (dotted line). **b** Light-induced FTIR difference spectrum corresponding to $Tyr_D$ oxidation in Photosystem II. Negative bands correspond to the dark adapted resting state, while the positive bands correspond to the light-induced $Tyr_D^{\bullet}$ state (Hienerwadel et al. 1996)

1986; Venyaminov and Kalnin 1990b), corresponding to different hydrogen bonding patterns and electrostatic interactions of the peptide carbonyl groups in these structures. The structural analysis of proteins thus largely involves IR spectroscopy, notably to inspect the effect of temperature on protein folding (Hauser et al. 2008; Mukherjee et al. 2008) or the consequences of protein–protein interactions (Karyakin et al. 2007).

Water also contributes with two main bands in the mid-infrared: the intense OH stretching mode, $\nu$(OH), between 3,600 and 3,100 $cm^{-1}$ and the HOH bending mode, $\delta$(HOH), at $\approx$ 1645 $cm^{-1}$ (Fig. 2a). The $\nu$(OH) mode, which is sensitive to hydrogen bonding properties of water molecules, has been used to analyze water molecules at the active sites of bacterhiorhodopsin and Photosystem II (see Section 'Properties and role of water molecules'). The absorption coefficient of the $\nu$(OH) mode is such that the IR detector is saturated in the 3,600–3,100 $cm^{-1}$ region for an aqueous sample of even less than 10 μm path length. Partially dehydrated samples must be used to identify the role of specific water molecules at protein active sites. Similarly, the absorption of an aqueous sample with 10 μm path length is above 1 absorption unit at 1,645 $cm^{-1}$; thus, it is too high to obtain reliable FTIR spectra. This is a strong limitation for the analysis of samples in aqueous solutions. Thin samples, with protein concentrations in the millimolar range, or partially dried protein films have been used for transmission infrared spectroscopy in water. Protein structure analysis using the properties of the Amide I band often involves samples in $^2H_2O$: indeed, the $\delta(^2HO^2H)$ mode contributes at $\approx$1,200 $cm^{-1}$ and does not impair the analysis of the Amide I band at 1,680–1,620 $cm^{-1}$.

Amino acid side chains have a number of characteristic normal modes in the mid infrared (Venyaminov and Kalnin 1990a; Barth 2007). This is exemplified for aspartate or glutamate side chains. The protonated carboxylic groups are characterized by the $\nu$(C=O) mode, which occurs above 1,680 $cm^{-1}$ and is sensitive to hydrogen bonding interactions and to the environment polarity. For a hydrogen bonded COOH group, the $\nu$(C=O) mode is downshifted by up to 10 $cm^{-1}$ upon $H_2O/^2H_2O$ exchange; this is often used as a diagnostic tool for such hydrogen bonding interactions in proteins. In contrast, the deprotonated carboxylate groups have typical $\nu_{as}(COO^-)$ and $\nu_s(COO^-)$ modes at 1,580–1,560 and 1,420–1,395 $cm^{-1}$, respectively. These modes are also sensitive to the carboxylate environment. Upon carboxylate binding to a metal ion, the frequency difference ($\nu_{as} - \nu_s$) is usually altered as compared to the typical frequency difference observed in solution. The parameter ($\nu_{as} - \nu_s$) is smaller for a bidentate carboxylate ligand and greater in the case of a monodentate ligand (Deacon and Phillips 1980; Nakamoto 1997). This example illustrates a specific interest of infrared spectroscopy to directly probe the protonation state of aspartate or glutamate groups, and hence their involvement in proton transfer pathways, and to study their properties as metal–ligands in proteins.

Other amino acids, and notably tyrosine, arginine or histidine have typical vibrations, which have been useful in identifying their contributions to infrared spectra and their properties in various proteins. The hydrogen bonding properties of the two redox-active tyrosines of Photosystem II (PS II) have been analyzed in the reduced and oxidized states using FTIR difference spectroscopy (Hienerwadel et al. 1997, 2008; Noguchi et al. 1997; Berthomieu and Hienerwadel 2005). IR bands of histidine side chains are sensitive to the protonation state of the imidazole side chain as well as sensitive to metal-binding (Hasegawa et al. 2000, 2002; Dupeyrat et al. 2004, and references therein). These IR markers have been used to analyze histidine properties as a ligand of (bacterio)chlorophylls (Breton et al. 2002) or of Mn and the non-heme iron in Photosystem II (Hienerwadel and Berthomieu 1995; Noguchi et al. 1999; Yamanari et al. 2004; Kimura et al. 2005).

## FTIR difference spectroscopy

### *Sample preparation*

The strong absorption of water and of the peptide bonds dominates the absorption spectrum of protein aqueous samples. The samples thus consist of concentrated protein solutions placed in measuring cells formed by two IR transparent windows[4] separated by a path length smaller than 10 μm. Dried films of bacterial reaction centers or Photosystem I (PSI) have been used. For PSII, either a pellet of PSII enriched membranes is squeezed between two windows, or concentrated solutions of PSII core complexes are partially dried on a window. The hydration level can be controlled by the deposition of a small volume of a water–glycerol mixture at a defined water/glycerol ratio in the sample chamber formed by the two tightly sealed IR windows (Noguchi and Sugiura 2002a).

In order to analyze an active site in a protein at the molecular level, FTIR difference spectroscopy must be used. This approach couples the specific perturbation of the active site of interest with the recording of absorption spectra of the sample before and after the perturbation. The difference spectrum resulting from the subtraction of these two spectra contains contributions from the amino acids

[4] IR transparent materials must be used. For the mid-IR domain, calcium fluoride is a material of choice for its moderate hygroscopic character.

and cofactors selectively perturbed. Such a difference spectrum shows a large number of small signals which correspond to single vibrations (Fig. 2b). It is, therefore, of great help to be able to perform the reaction repeatedly on the same sample, to average data from several cycles and thus increase the signal to noise. Indeed, very small bands are observed in FTIR difference spectra ($10^{-5}$–$10^{-3}$ a.u.), notably for large proteins such as PSII.

*Light-induced FTIR difference spectroscopy*

This approach was first developed on bacteriorhodopsin, using light as a trigger of the photochemical cycle (Br → M transition, Rothschild et al. 1981). The control of the photo-induced reaction can be done (i) kinetically, by recording the spectrum during a short time after a light-flash or by using time-resolved FTIR difference spectroscopy; (ii) by controlling the sample temperature; (iii) by using chemicals (electron donors and/or electron acceptors, reducing or oxidizing agents) to poise a light-induced reaction intermediate. Time-resolved FTIR spectroscopy involves rapid scan techniques, with 10–25 ms time resolution (Thibodeau et al. 1990) or step-scan FTIR spectroscopy (Weidlich and Siebert 1993) with time resolution in the μs to ns range (Mezzetti et al. 2003; Kötting and Gerwert 2005; Sivakumar et al. 2005). In addition, time-resolved IR spectroscopy can be achieved using tunable infrared laser diodes (Hienerwadel et al. 1990, 1995). For time resolved techniques, and especially for step-scan techniques, the reaction must remain unchanged for a high number of repetitive flashes. This restricts the use of this technique to very stable reactions and step-scan techniques are not easy to apply to photosynthetic reactions centers, notably PSII.

It is also very important to generate the same reaction-induced state in all the active centers of the protein, to obtain reliable FTIR difference spectra. In this respect, the use of alternate spectroscopic controls (UV–Visible, EPR) is often essential to validate the experimental conditions (Hienerwadel and Berthomieu 1995; Hienerwadel et al. 1996). Thus, FTIR difference spectroscopy is seldom used to identify a new reaction state, but it is very useful to analyze the details of the molecular properties of this state.

The use of photolabile precursor compounds such as caged ATP or caged-calcium was implemented to trigger light-induced reactions of $Ca^{2+}$-ATPases or changes in sarcoplasmic reticulum (Barth et al. 1990; Buchet et al. 1991). The ATP molecule is released from the inactive precursor by a photolytic UV flash, and then it interacts with the protein. A number of caged compounds or light-sensitive molecules are now available, which could be used for infrared spectroscopy (Barth and Corrie 2002; Mayer and Heckel 2006). UV-light excitation was also used to form radicals of aromatic amino acids and notably tyrosine, 4-methylimidazole, and phenol at low temperature in vitro (Berthomieu and Boussac 1995; Berthomieu et al. 1998a; Ayala et al. 2002).

*Electrochemically-induced FTIR difference spectroscopy*

FTIR-difference spectroscopy has been generalized to a broader range of proteins, by the implementation of other means to trigger a reaction. Electrochemistry coupled to FTIR difference spectroscopy allows us to probe all proteins with redox-centers. In the area of photosynthesis, it was first used to study the IR properties of isolated redox chlorophyll, quinone and heme cofactors. Indeed, a way to identify the contributions from cofactors in the complex FTIR difference spectra recorded with protein samples involves the comparison with spectra of isolated model compounds. Thin path-length transmission cells were developed to analyze model compounds in solvents (Mäntele et al. 1988a, b; Bauscher et al. 1990), as well as model compounds and proteins in aqueous solutions (Moss et al. 1990; Leonhard and Mäntele 1993; Berthomieu et al. 2006). In these cells, the working electrode is a gold grid (4–7 μm thick) deposited between two visible and infrared transparent windows ($CaF_2$, or chemical vapor deposition (CVD) diamond). In the cells for aqueous samples, the path-length is below 10 μm, the sample volume is less than 10 μl, but the concentration of proteins is high, up to the millimolar range. An electrochemical cell has also been developed for ATR (attenuated total reflection)-FTIR spectroscopy (Rich and Iwaki 2007).

*Perfusion-induced ATR-FTIR difference spectroscopy*

New approaches for FTIR difference spectroscopy involve the use of ATR, coupled with the perfusion of samples with buffers containing a triggering reagent or a metal cofactor (see Rich and Iwaki (2007) for a review). With an ATR setup, the infrared beam is reflected within the ATR crystal. At each reflection, the evanescent wave probes a layer of the sample deposited on the crystal, within a thickness of about 1 μm. In contrast with transmission FTIR difference spectroscopy, in which reactions must be induced in the thin path length sample by external methods, without modifying the sample volume and content, this approach has the advantage of minimizing global absorption changes, when the protein layer deposited on the ATR crystal is exposed to reactants administrated at the top of the sample. This approach was applied to the recording of FTIR difference spectra of different redox cofactors of PSI or bacterial reaction centers dried as stable films on the ATR crystal (Iwaki et al. 2002). The difference spectra obtained by the perfusion of buffers poised at different

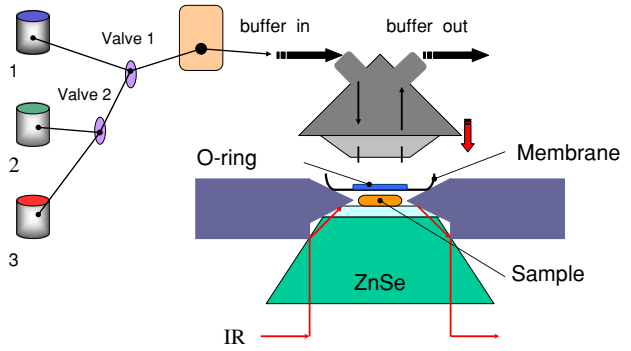


**Fig. 3** Scheme of the attenuated total reflection (ATR)-microdialysis setup allowing the perfusion of a protein sample by three different buffers

redox potentials were identical to spectra recorded using light-induced FTIR difference spectroscopy (Iwaki et al. 2002). This approach was also extended to the analysis of soluble proteins maintained on the ATR crystal by a dialysis membrane (Lehmann et al. 2002; Gourion-Arsiquaud et al. 2005; see Fig. 3). For this latter application, it is of prime importance to maintain a constant protein concentration on the ATR crystal, and to minimize the reaction time. This was achieved by the setup of a microdialysis chamber (Gourion-Arsiquaud et al. 2005; Rich and Iwaki 2007; Vidaud et al. 2007), which contains less than 5 µl of sample. Two or three buffers can be perfused subsequently through the sample, using a peristaltic pump and two three-way valves, monitored by the FTIR spectrometer. With such a miniaturized system, IR changes corresponding to single modes are detected (Fig. 3).

With the above-described reaction-induced techniques, protein–protein interactions, as well as cofactor–protein interactions and protein metal-binding sites can be studied in a wide range of soluble or membrane proteins.

## Band assignments

### *Comparison with spectra of model compounds*

Comparison of spectra recorded with protein samples and spectra recorded on model compounds is a usual approach to identify the contributions from cofactors or amino acid side chains in the protein and to discover precise specific structures or interactions.

The IR contributions of bacteriochlorophyll cofactors in the complex $P^+Q_A^-/PQ_A$ or $P^+/P$ FTIR difference spectra recorded with reaction centers from purple bacteria were first analyzed by comparison with electrochemically induced FTIR spectra of neutral and cationic bacteriochlorophyll (BChl, $BChl^+/BChl$ difference spectra) in organic solvents of different polarity (Mäntele et al. 1988a, b; Leonhard and Mäntele 1993). This approach allowed the assignment of 10a ester and 9 keto C = O groups of the neutral and cationic forms of bacteriochlorophylls. Similarly, the contributions from chlorophyll 9keto and 10a ester C=O groups in the primary electron donor ($P_{700}$) of PSI were identified by comparison of the light-induced $P_{700}^+/P_{700}$ spectra with electrochemically induced (pyro)chlorophyll$^+$/chlorophyll difference spectra in tetrahydrofurane (Nabedryk et al. 1990a), as well as by using site-directed mutants (Hastings et al. 2001). The frequency of the (bacterio)chlorophyll IR modes allowed the analysis of their hydrogen bonding properties and the extent of charge delocalization in primary electron donors of the different photosystems (Noguchi et al. 1998; Breton 2001; Pantelidou et al. 2004).

Similar approaches combining light-induced spectroscopy on photosynthetic reaction centers and electrochemically generated difference spectra on models were used to assign the IR contributions of quinones in photosynthetic reaction centers (Bauscher et al. 1990; Nabedryk et al. 1990b), or to analyze the high and low potential forms of cytochrome b559 (Berthomieu et al. 1992). A chemically generated $\beta$-carotene cation in chloroform was used to identify the contribution of a carotenoïd cation in light-induced FTIR difference spectra recorded at low temperature in PSII (Noguchi et al. 1994).

Absorption spectra of model compounds are also used to assign vibrational modes from amino acid side chains in proteins. This has notably been done to identify IR contributions from aspartate, glutamate, tyrosines or histidines and to identify their hydrogen bonding properties or the role of histidine as metal ligand. IR markers of histidine–metal interactions have been analyzed notably using 4(5)-methylimidazole as a model (Dupeyrat et al. 2004, and references therein). As also observed by resonance Raman spectroscopy (see B. Robert, this issue), the $\nu(C_4C_5)$ mode frequency and its sensitivity to $H/^2H$ exchange differ for metal complexes in which methylimidazole binds via the N$\tau$ or N$\pi$ imidazole nitrogens. The ring $\nu$(C5 N$\tau$) mode of 4(5)-methylimidazole contributing at $\approx$1,100 cm$^{-1}$ is strongly enhanced upon metal binding (Berthomieu et al. 1992; Dupeyrat et al. 2004). This band, downshifted by $\approx$7 cm$^{-1}$ upon $^{15}$N labeling, has been observed in a number of proteins and is a useful IR marker of histidine–metal coordination.

### *Theoretical approaches for normal modes calculations*

Experimental data on model compounds are being increasingly analyzed using theoretical approaches to predict normal mode frequencies. Calculations based on density functional methods give satisfactory normal mode predictions. The combined experimental and theoretical approaches are very powerful in correlating the mode frequencies with specific structures or interactions within the

protein. As an example, the theoretical analysis of the influence of different types of hydrogen bonding interactions (proton donor, proton acceptor, or both) on the IR frequency of tyrosine side-chain modes (Takahashi and Noguchi 2007) has been useful in interpreting FTIR data recorded on $Tyr_D$ in PSII (Hienerwadel et al. 2008; also see below). Similarly, ab initio normal mode predictions were used to better understand the modulation of the *v*(CO) IR mode frequency of tyrosinyl radicals as a function of hydrogen bonding interactions (O'Malley 2002). Other examples concern the normal mode analysis of 4(5)-methylimidazole, a model of the histidine side chain, in different protonation states or as metal ligand (Hasegawa et al. 2000, 2002, and references therein) or the analysis of the hydrogen bonding status of protonated side chains from aspartate and glutamate (Nie et al. 2005).

*Isotope labeling*

Studies on model compounds of both cofactors and amino acid side chains often imply the use of isotope labeling. Isotope labeling not only enables band assignments but also helps to determine specific normal modes of vibration, which contain structural information. The same labeling experiments can be performed on models and in the protein sample, either by substitution of the cofactor (quinones) or by introducing a labeled precursor in the culture media for biosynthetic incorporation (hemes or chlorophylls). Labeling of the protein itself is obtained by growing the bacteria in a synthetic medium containing either a labeled carbon or nitrogen source (global $^{13}C$ or $^{15}N$ labelling) or the labelled amino acid (e.g., tyrosine or histidine). Isotope edited FTIR spectroscopy has been increasingly used not only to analyze properties of amino acid side chains but also to probe the structure of proteins with high precision.

The substitution of cofactors by chemically modified or isotope labelled cofactors is a powerful means to selectively perturb the FTIR spectrum. As an example, the primary ($Q_A$) and secondary ($Q_B$) quinones of the bacterial reaction centers of *R. sphaeroides* and *B. viridis* have been substituted by site-specific isotopically labeled quinones. For $Q_A$, the $^{18}O$ labelling on both carbonyl oxygens allowed the identification of two very different *v*(C=O) frequencies, showing an asymmetric hydrogen bonding pattern for the two carbonyl groups in the bacterial RC (Breton et al. 1994a). Site-specific $^{13}C$ labeling, on either one of the two carbonyls, or at each carbon positions in the quinone ring, allowed the assignment of the strong hydrogen bond to the carbonyl group distal to the quinone isoprenoid chain (Breton et al. 1994b; Brudler et al. 1994). In contrast, for the semiquinone $Q_A^-$, similar hydrogen bonding interactions were proposed for the two C$\underline{\circ\circ}$O bonds (Breton et al. 1994b; Brudler et al. 1994). For both

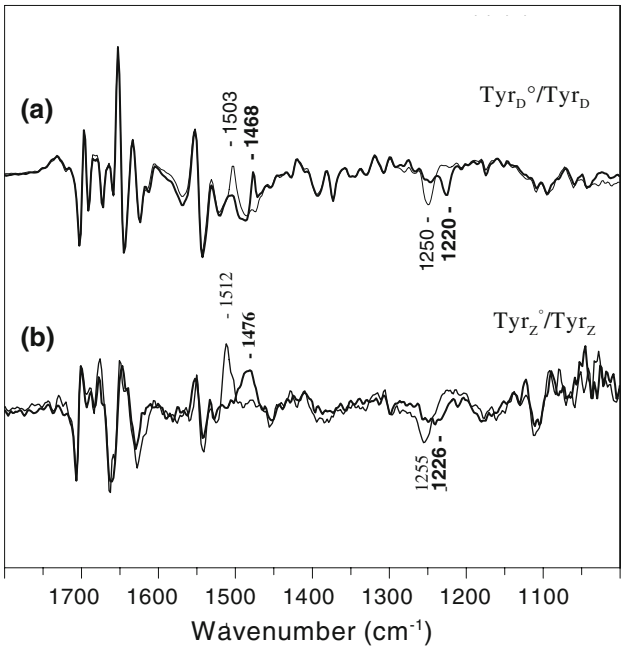


**Fig. 4** Light-induced FTIR difference spectra corresponding to the oxidation of redox-active $Tyr_D$ (**a**) and $Tyr_Z$ (**b**) of Photosystem II (Hienerwadel et al. 1997; Berthomieu et al. 1998a, b). Spectra were recorded using PSII core complexes of *Synechocystis sp.* PCC 6803 with unlabeled tyrosines (thin lines) or tyrosines $^{13}C$ labeled at the ring carbon involved in the C–O bond (thick lines)

$Q_B$ and $Q_B^-$, the use of isotopically labeled quinones showed that the two quinone oxygen atoms are involved in moderate hydrogen bonds (Breton et al. 1995; Brudler et al. 1995). Thus, in addition to a precise assignment of quinone vibrations, detailed structural analysis could be made, concerning the hydrogen bonding pattern at the carbonyl groups and also concerning steric constraints exerted by the protein on quinone substituents (Breton et al. 1995).

The specific isotope labeling of amino acids has also proven useful for a number of spectroscopic techniques as ESEEM (electron spin echo envelope modulation), ENDOR (electron nuclear double resonance) or FTIR spectroscopy. As an example, this strategy has been used to study the vibrational properties of two redox active tyrosines ($Tyr_D$ and $Tyr_Z$) of PSII, using reaction centers of *Synechocystis* sp. PCC 6803 with labeled tyrosines (Hienerwadel et al. 1997; Noguchi et al. 1997; Berthomieu et al. 1998b). $^{13}C$-labeling at the phenolic $C_4$ carbon atom only led to the shift of one negative band for reduced $Tyr_D$ (or $Tyr_Z$) and one positive band for oxidized $Tyr_D^{\bullet}$ (or $Tyr_Z^{\bullet}$; see Fig. 4). This labeling allowed the unambiguous assignment of these bands to the phenol C–O group of reduced and oxidized tyrosines.

*Site-directed mutagenesis*

Protein bands can also be identified by the comparison of spectra recorded with wild type and site-directed mutant

proteins. This approach has been often used and some examples are illustrated in the following section. Special care must be taken to differentiate between the direct and indirect effects of the mutation. The IR contributions of the native amino acid disappear in the mutant. However, the mutation can slightly alter the protein structure leading to band shifts or spectral changes in the spectra. The combination of site-directed mutagenesis and isotope labeling is also powerful in detailed structural information (see below).

## Typical information gained using FTIR difference spectroscopy of photosystems

### Conformational changes

FTIR difference spectroscopy is very sensitive to detect conformational changes in proteins, because of the strong IR absorption of peptide carbonyl groups. However, one striking information obtained from the first comparison of light-induced FTIR difference spectra recorded on bacterial reaction center with redox-induced spectra of isolated cofactors was that the charge separation induced the perturbation of only a few protein carbonyl groups (Mäntele et al. 1988a). This holds true for a large number of light-induced reactions in bacterial reaction centers and photosystems.

### Hydrogen bonding interactions of cofactors and redox intermediates

FTIR spectroscopy is not the only technique which allows the detection of hydrogen bonding interactions on the various cofactors in the reaction centers. ENDOR and ESEEM also give precise analysis of interactions involving singles atoms in a molecule. However, these techniques can only probe radical species, i.e., the oxidized or reduced intermediates of the reaction. They do not provide information on the fine structure of the cofactors in the resting state. We have illustrated above how the use of specific isotope labeling of the quinones revealed the hydrogen bonding interactions of $Q_A$ and $Q_B$ in the dark-adapted resting state of the bacterial reaction center. This approach, coupled with the analysis of FTIR difference spectra obtained with site directed mutants, further showed that only one $Q_B$ binding site was observed in the FTIR samples. These results contrasted with crystallographic studies that proposed two -distal and proximal- locations for $Q_B$. They showed that all $Q_B$ molecules involved in electron transfer from $Q_A^-$ were located at the proximal binding site (reviewed in Nabedryk and Breton 2008).

Another example is the analysis of hydrogen bonding interactions formed by reduced $Tyr_D$ in Mn-depleted photosystem II. In PSII reaction centers of *Synechocystis sp*. PCC 6803, the rate of oxidation of $Tyr_D$ dramatically increases as a function of pH, with a behavior corresponding to a pKa of $\approx$7.6 (Faller et al. 2001). The origin of the group(s) responsible for this apparent p*K*a was unknown. The analysis of $Tyr_D^{\bullet}/Tyr_D$ FTIR difference spectra on wild type (WT) PSII and PSII with $^{13}$C-labeled tyrosines at different pHs showed that the pH-induced change concerns the reduced $Tyr_D$-state only, and reduced $Tyr_D$ itself (Hienerwadel et al. 2008). However, the frequencies of the $Tyr_D$ IR modes showed that $Tyr_D$ does not deprotonate at pH higher than 7.6, but forms a stronger hydrogen bond, acting as hydrogen bond donor only. At pH below 7.5, the IR frequencies observed for $Tyr_D$ indicate that it could be involved both as a hydrogen bond donor and acceptor, as judged by a comparison with calculations performed on models by Takahashi and Noguchi (2007). The involvement of $Tyr_D$ in a strong hydrogen-bonding interaction correlates with the ability to oxidize $Tyr_D$ rapidly at room temperature. This example illustrates the high precision that can be obtained using FTIR spectroscopy in the analysis of amino acid side chain properties.

### Proton transfer coupled to electron transfer: direct probe of Asp and Glu protonation state

In bacterial reaction centers and PSII, the secondary electron acceptor $Q_B$ is doubly reduced and protonated to form the quinol $Q_BH_2$ which leaves the reaction center. These reactions involve proton transfers across the protein towards $Q_B$, which are coupled to sequential electron transfers from $Q_A^-$.

FTIR spectroscopy is the method of choice to probe directly protonation changes of aspartate and glutamate side chains, by following absorption changes of the $\nu$(C = O) mode of the protonated carboxylic (COOH) groups in the 1,770–1,700 cm$^{-1}$ region.[5] This approach has been used to determine the role of Asp and Glu residues located near $Q_B$ in proton uptake upon $Q_B^-$ formation in bacterial reaction centers (reviewed in Nabedryk and Breton 2008). In the first experiments using time-resolved IR (Hienerwadel et al. 1995; see Fig. 5) and FTIR (Nabedryk et al. 1995) spectroscopy on WT and GluL212Gln mutant reaction centers of *Rb. sphaeroides,* the authors assigned a positive band at 1,728 cm$^{-1}$ to the protonation of a fraction of GluL212 side chain upon $Q_B^-$ formation at pH 7. Indeed, the 1,728 cm$^{-1}$ band was downshifted by $\approx$10 cm$^{-1}$ upon H/$^2$H exchange (typical shift for a COOH group exchangeable with the

[5] In contrast, the identification of the $\nu_{as}$ and $\nu_s$ ($COO^-$) modes of the corresponding carboxylate forms is often impaired by many other superimposed IR modes in the 1,610–1,550 and 1,420–1,380 cm$^{-1}$ region. Isotope labeling is useful in identifying these modes.

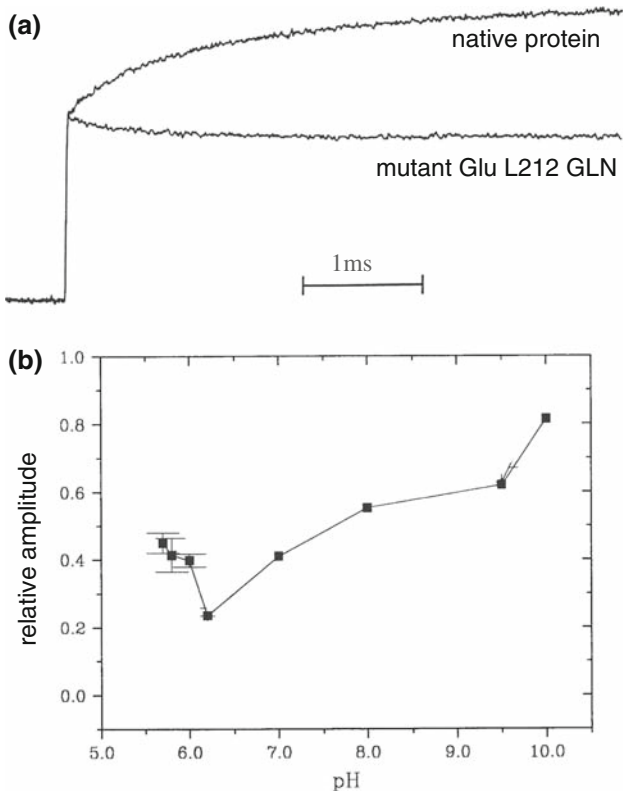


**Fig. 5** **a** Time resolved IR changes recorded at 1725 $cm^{-1}$ with reaction centers from *Rb. sphaeroides* WT (wild type, native protein) and GluL212Gln mutant (Hienerwadel et al. 1995). **b** IR amplitude of the slow phase component corresponding to the proton uptake as a function of pH

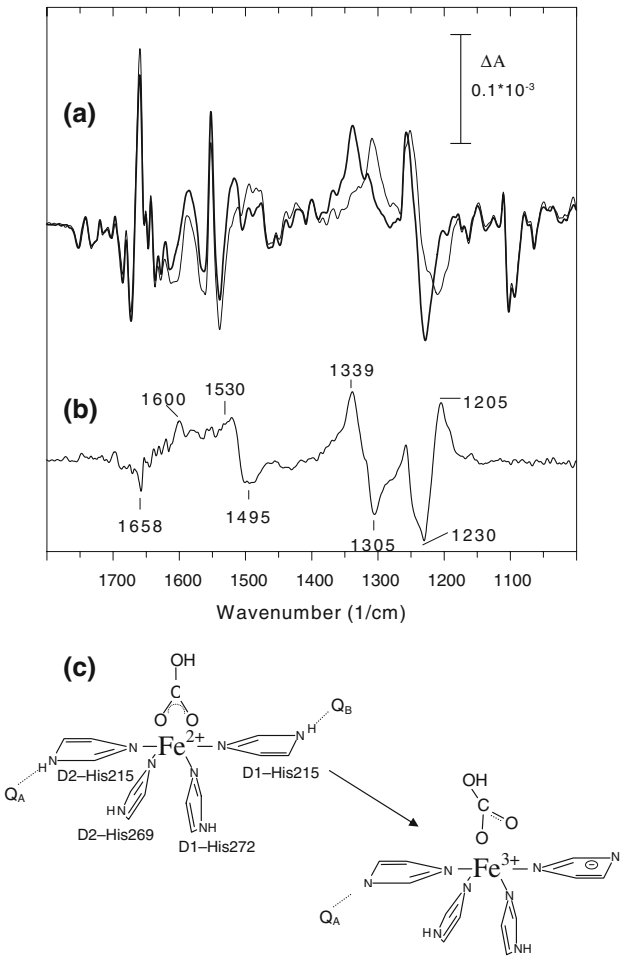


**Fig. 6** **a** Light-induced $Fe^{2+}/Fe^{3+}$ FTIR difference spectra recorded with Photosystem II enriched membranes of spinach in the presence of $^{12}C$-bicarbonate (thin line) or $^{13}C$-labeled bicarbonate (thick line). **b** $^{12}C$-minus-$^{13}C$ difference spectrum calculated from the spectra in A; **c** structural changes upon Fe oxidation resulting from the interpretation of the FTIR data

solvent) and disappeared in the GluL212Gln mutant (Fig. 5). The time resolved study also showed that the proton uptake by GluL212 occurred in a broad pH range (pH 6–10). These results were in disagreement with the interpretation of pH dependence of electron transfer rate or proton uptake experiments on WT and mutants that suggested proton uptake by GluL212 at high pH only. However, the proton transfer mechanisms associated with $Q_B^-$ formation is a typical example, where the interpretation of global effects is complicated by strong interactions between several groups. In IR spectroscopy, each residue has its own and single signature. Therefore, this technique is particularly suited to analyze such complex situations (Nabedryk and Breton 2008). Further experiments on a large number of mutants confirmed that GluL212 was responsible for the IR band at 1,728 $cm^{-1}$, and that it was the only carboxylic group getting partially protonated upon $Q_B^-$ formation at pH 4–11 (Nabedryk and Breton 2008).

## Identification and properties of metal ligands

The sensitivity of vibrational modes of amino acid side chain groups to interactions with metals can be used to identify amino acid metal ligands and to analyze the properties of metal–ligand interactions. This is illustrated by the detailed analysis of the correlation between the mode of binding of carboxylate groups to metals and the frequency of the asymmetric ($\nu_{as}$) and symmetric ($\nu_s$) stretching mode frequencies (Deacon and Phillips 1980; Nakamoto 1997).

This property was used to propose that bicarbonate is a bidentate ligand of the non heme iron of PSII in the $Fe^{2+}$ state (see Fig. 6; Hienerwadel and Berthomieu 1995). In this study, light-induced $Fe^{2+}/Fe^{3+}$ FTIR difference spectra recorded with samples containing unlabeled or $^{13}C$-labeled bicarbonate were compared to allow an unambiguous assignment of the bicarbonate IR modes. Indeed, the superimposition of the two spectra (Fig. 6a) shows that only a few IR bands appear at different frequencies in these two spectra. These bands are bicarbonate IR modes both sensitive to bicarbonate $^{13}C$-labeling and to the change in

redox state of the non-heme iron. The assignment of these IR bands, extracted in the $^{12}$C-minus-$^{13}$C difference spectrum (Fig. 6b), was done considering that a downshift of the bicarbonate IR modes is expected upon bicarbonate $^{13}$C-labeling. The two bands at 1,530 and 1,338 cm$^{-1}$ were assigned to the $\nu_{as}$ and $\nu_s$ ($COO^-$) modes of bicarbonate in the $Fe^{2+}$ state. The frequency difference of 192 cm$^{-1}$ is lower than that observed for bicarbonate in solution ($\approx$285 cm$^{-1}$), leading to the conclusion that bicarbonate is a bidentate ligand of $Fe^{2+}$ (see Hienerwadel and Berthomieu 1995 for the details in assignment). In the $Fe^{3+}$-state, the bicarbonate $\nu_{as}$ and $\nu_s$ ($COO^-$) modes were identified at 1,658 and 1,230 cm$^{-1}$. These frequencies indicate that bicarbonate is a monodentate ligand of $Fe^{3+}$ (Fig. 6b). These data support the extensive work of Govindjee and coworkers that show that bicarbonate plays an essential role in the electron and proton transport in the $Q_A$ $Q_B$ region of PSII (see e.g., Van Rensen et al. 1999; Rose et al. 2008).

For PSII, one main challenge is the elucidation of the molecular mechanism of water oxidation at the $Mn_4Ca$ active site (see Wydrzynski and Satoh 2005). In this respect, FTIR difference spectroscopy plays a central role in identifying the Mn–ligands and the changes in ligand–Mn (ligand–Ca) interactions during the sequential steps leading to water oxidation. This is challenging in the context where the three dimensional X-ray structures most probably do not correspond to physiological oxidation states of the Mn cluster. Details of the results obtained using FTIR difference spectroscopy of the oxygen evolving complex are given in several reviews (Noguchi and Berthomieu 2005; Noguchi 2007; Debus 2008,). In particular, the use of universal $^{13}$C and $^{15}$N labeling allowed the identification of a number of carboxylate groups: the $\nu_{as}$ and $\nu_s$ ($COO^-$) modes were identified by their large sensitivity to $^{13}$C-labeling (25–50 cm$^{-1}$ downshifts) and their insensitivity to $^{15}$N labeling (Noguchi and Sugiura 2003; Yamanari et al. 2004). Comparison of spectra recorded with native PSII and PSII depleted of calcium further showed the disappearance of band pairs at 1,587 cm$^{-1}$ ($S_2$-state)/1,560 cm$^{-1}$ ($S_1$-state) and 1,364 cm$^{-1}$ ($S_2$-state)/1,403 cm$^{-1}$ ($S_1$-state), which were assigned to the $\nu_{as}$ and $\nu_s$ ($COO^-$) modes of a single carboxylate group. As discussed above for bicarbonate, the $\nu_{as} - \nu_s$ frequency differences of 157 cm$^{-1}$ in the $S_1$ state and of 223 cm$^{-1}$ in the $S_2$ state were taken as indicative of a drastic change in coordination of this carboxylate—from bridging to unidentate coordination—to a Mn of the oxygen evolving complex (Noguchi et al. 1995). The assignment of each carbonyl group to a specific amino acid involves now the use of site directed mutants sometimes in combination with specific isotope labeling (Chu et al. 2004; Strickler et al. 2006, 2007; see reviews by Debus 2008 and Noguchi 2008).

We have previously shown that the IR modes of histidine can also be used to identify its role as a metal ligand. Signals at 1,102 and 1,094 cm$^{-1}$, sensitive to $^{15}$N-labeling, were detected in the $Fe^{3+}$ state of the non-heme iron of PSII (Fig. 6a; Hienerwadel and Berthomieu 1995) and therefore assigned to histidine ligands of the iron. The band at 1,094 cm$^{-1}$ was perturbed upon *o*-phenanthroline binding at the $Q_B$ binding site, strongly suggesting that it is due to D1-His215 (Fig. 6c; Berthomieu and Hienerwadel 2001). The frequency of the His 1,094 cm$^{-1}$ band was taken as indicative of deprotonation of the histidine side chain upon iron oxidation, as illustrated by the reaction model proposed in Fig. 6c.

IR contributions at $\approx$1,114 cm$^{-1}$ in the spectra of S-state transitions, sensitive to $^{15}$N-labeling, were also assigned to one histidine ligand of Mn, possibly D1His332 (Noguchi et al. 1999; Yamanari et al. 2004; Kimura et al. 2005). This histidine is observed in the $S_0$–$S_1$, $S_1$–$S_2$ and $S_2$–$S_3$ S-states transitions. The effect of deuteration on that mode was taken as indirect evidence that this histidine ligates the Mn by the imidazole N$\tau$ nitrogen (Noguchi et al. 1999).

## Properties and role of water molecules

A particularly attractive possibility of FTIR spectroscopy is the direct analysis of internal water molecules with active roles in proton transfer or in catalysis in proteins. Such water molecules are present in bacteriorhodopsin, bacterial reaction centers, and in PSII. For the latter system, the direct probing of substrate water during water oxidation at the oxygen evolving center is appealing.

The water molecules can be directly probed by their $\nu$(OH) modes in reaction-induced FTIR difference spectra. This is, however, challenging due to the large background absorption of the water in the sample suspension. The study of water molecules has been undertaken at low temperatures (Yamazaki et al. 1995; Kandori 2000; Noguchi and Sugiura 2000) or on partially dehydrated protein films at the room temperature (Noguchi and Sugiura 2002; Lorenz-Fonfria et al. 2008).

The broad absorption of water or ice prevents analysis of the 3,500–3,000 cm$^{-1}$ range. However, at low temperatures, the sample absorption is very stable and the difference bands flanking this region are detected in light-induced FTIR difference spectra. At the room temperature, partial dehydration of the protein sample is controlled by the addition of droplets of water/glycerol mixtures in proximity of the protein film, placed in a tight measurement cell (Noguchi and Sugiura 2002a). The water/glycerol ratio determines the humidity of the cell and hence of the protein film. Using this approach, Noguchi and Sugiura (2002b) have identified contributions from water molecules

during the S-state transitions of the oxygen evolving complex of PSII from *Synechococcus elongatus*. The assignment of the water bands resides on their sensitivity to $H_2O/H_2^{18}O$ exchange. Bands observed at 3,618 $cm^{-1}$ ($S_2$-state) and 3,585 $cm^{-1}$ ($S_1$-state) were thus assigned to a water molecule sensitive to Mn oxidation during the $S_1$ to $S_2$ transition of the water oxidizing complex.

The *v*(OH) mode frequency strongly depends on hydrogen bonding interactions. Moreover, for water molecules involved in symmetric interactions, the two *v*(OH) vibrations are coupled, resulting in an asymmetric and in a symmetric mode. In contrast, water molecules involved in asymmetric interactions have two uncoupled *v*(OH) modes at different frequencies. To measure the extent of intramolecular coupling of the water molecules, samples in $H_2O$ are compared with samples in 50% of $H_2O$ and 50% $^2H_2O$: for the $HO^2H$ molecules, the *v*(OH) mode is decoupled from the *v*($O^2H$) mode. The shift of the *v*(OH) modes resulting from this decoupling provides us information on the degree of asymmetry of the water molecule: a large shift corresponds to water molecules with a strong intramolecular coupling, i.e., involved in symmetric interactions, while a small shift corresponds to water molecules involved in asymmetric interactions, i.e., with only one hydrogen involved in a strong hydrogen bond or electrostatic interaction.

Using this strategy, Noguchi and Sugiura (2000) concluded that bands at 3,618 ($S_2$-state) and 3,585 ($S_1$-state) $cm^{-1}$ in the $S_2/S_1$ FTIR difference spectra correspond to an asymmetric water molecule, with one OH group strongly hydrogen-bonded, and that this asymmetry increases upon $S_1$ to $S_2$ transition. Noguchi and Sugiura (2000) proposed that this molecule is substrate water, which could be coordinated to Mn. Similarly, absorption changes of two water molecules were observed upon $Tyr_D$ oxidation in PSII from *Thermosynechococcus elongatus* (Takahashi et al. 2007). The modest shift, observed upon partial water $^2H$ labeling, led to the conclusion that the water molecules are involved in asymmetric hydrogen bonding interactions. It remains to be determined whether these water molecules are coupled to $Tyr_D$ directly or via a hydrogen bonding network around $Tyr_D$.

## Conclusions

We have shown in this review that infrared spectroscopy provides a means to have a look at structural details for proteins in solution with spatial and temporal resolution greater than in most of the available crystallographic data. Infrared spectroscopy is unique to probe amino acid side chains and water molecules, as well as cofactors in redox states, which are silent in other spectroscopic techniques. Therefore, although this technique requires well defined experimental conditions and the use of site directed mutants or isotope labeling, it will continue to play a key role in the analysis of photosystems and other proteins, and notably to unravel the mechanism of water oxidation in PSII.

The remarkable increase in the number of publications on proteins involving (FT)IR spectroscopy shows the important and specific role of this technique. The continuous development of new and complementary experimental strategies and theoretical approaches opens its field of application in various research areas.

**Acknowledgment** This manuscript was edited by Govindjee.

## References

Ayala I, Range K, York D, Barry BA (2002) Spectroscopic properties of tyrosyl radicals in dipeptides. J Am Chem Soc 124:5496–5505

Barth A (2000) The infrared absorption of amino acid side chains. Prog Biophys Mol Biol 74:141–173

Barth A (2007) Infrared spectroscopy of proteins. Biochim Biophys Acta 1767:1073–1101

Barth A, Corrie JE (2002) Characterization of a new caged proton capable of inducing large pH jumps. Biophys J 83:2864–2871

Barth A, Mantele W, Kreutz W (1990) Molecular changes in the sarcoplasmic reticulum $Ca^{2+}$ ATPase during catalytic activity: a Fourier transform infrared (FTIR) study using photolysis of caged ATP to trigger the reaction cycle. FEBS Lett 277:147–150

Bauscher M, Nabedryk E, Bagley K, Breton J, Mäntele W (1990) Investigation of models for photosynthetic electron acceptors. Infrared spectroelectrochemistry of ubiquinone and its anions. FEBS Lett 261:191–195

Berthomieu C, Boussac A (1995) FTIR and EPR study of radicals of aromatic amino acids, 4-methylimidazole and phenol generated by UV-irradiation. Biospectroscopy 1:187–206

Berthomieu C, Hienerwadel R (2001) Iron coordination in photosystem II: interaction between bicarbonate and the QB pocket studied by Fourier transform infrared spectroscopy. Biochemistry 40:4044–4052

Berthomieu C, Hienerwadel R (2005) Vibrational spectroscopy to study the properties of redox-active tyrosines in photosystem II and other proteins. Biochim Biophys Acta 1707:51–66

Berthomieu C, Boussac A, Mäntele W, Breton J, Nabedryk E (1992) Molecular changes following oxidoreduction of cytochrome b559 characterized by Fourier transform infrared spectroscopy and electron paramagnetic resonance: photooxidation in photosystem II and electrochemistry of isolated cytochrome b559 and iron protoporphyrin IX- bisimidazole model compounds. Biochemistry 31:11460–11471

Berthomieu C, Boullais C, Neumann JM, Boussac A (1998a) Effect of $^{13}C$, $^{18}O$, and $^2H$ labeling on the infrared modes of UV-induced phenoxyl radicals. Biochim Biophys Acta 1365:112–116

Berthomieu C, Hienerwadel R, Boussac A, Breton J, Diner BA (1998b) Hydrogen bonding of redox-active tyrosine Z of photosystem II probed by FTIR difference spectroscopy. Biochemistry 37:10547–10554

Berthomieu C, Marboutin L, Dupeyrat F, Bouyer P (2006) Electrochemically-induced FTIR difference spectroscopy in the mid to far infrared (200 μm) domain: a new setup for the analysis of metal-ligands in redox-proteins. Biopolymers 82:363–367

Breton J (2001) Fourier transform infrared spectroscopy of primary electron donors in type I photosynthetic reaction centers. Biochim Biophys Acta 1507:180–193

Breton J, Burie J-R, Berthomieu C, Berger G, Nabedryk E (1994a) The binding sites of quinones in photosynthetic bacterial reaction centers investigated by light-induced FTIR difference spectroscopy: assignment of the QA vibrations in *Rhodobacter sphaeroides* using $^{18}$O- or $^{13}$C- labeled ubiquinones and vitamin K1. Biochemistry 33:4953–4965

Breton J, Boullais C, Burie JR, Nabedryk E, Mioskowsky C (1994b) Binding sites of quinones in photosynthetic bacterial reaction centers investigated by light-induced FTIR difference spectroscopy: assignment of the interactions of each carbonyl of QA in *Rhodobacter sphaeroides* using site-specific $^{13}$C-labeled ubiquinone. Biochemistry 33:14378–14386

Breton J, Boullais C, Mioskowski C, Nabedryk E (1995) Binding sites of quinones in photosynthetic bacterial reaction centers investigated by light-induced FTIR difference spectroscopy: symmetry of the carbonyl interactions and close equivalence of the QB vibrations in *Rhodopseudomonas sphaeroides* and *Rhodobacter viridis* probed by isotope labeling. Biochemistry 34:11606–11616

Breton J, Xu W, Diner BA, Chitnis PR (2002) The two histidine axial ligands of the primary electron donor chlorophylls (P700) in photosystem I are similarly perturbed upon $P_{700}^{+}$ formation. Biochemistry 41:11200–11210

Brudler R, de Groot HJM, van Liemt WBS, Steggerda WF, Esmeijer R, Gast P, Hoff AJ, Lugtenburg J, Gerwert K (1994) Asymmetric binding of the 1- and 4-C=O groups of QA in *Rhodobacter sphaeroides* R26 reaction centers monitored by Fourier transform infra-red spectroscopy using site-specific isotopically labelled ubiquinone-10. EMBO J 13:5523–5530

Brudler R, de Groot HJM, van Liemt WBS, Gast R, Hoff AJ, Lugtenburg J, Gerwert K (1995) FTIR spectroscopy shows weak symmetric hydrogen bonding of the $Q_B$ carbonyl groups in *Rhodobacter sphaeroides* R26 reaction centers. FEBS Lett 370:88–92

Buchet R, Jona I, Martonosi A (1991) $Ca^{2+}$ release from caged-$Ca^{2+}$ alters the FTIR spectrum of sarcoplasmic reticulum. Biochim Biophys Acta 1069:209–217

Chu HA, Hillier W, Law NA, Babcock GT (2001) Vibrational spectroscopy of the oxygen-evolving complex and of manganese model compounds. Biochim Biophys Acta 1503:69–82

Chu HA, Hillier W, Debus RJ (2004) Evidence that the C-terminus of the D1 polypeptide of photosystem II is ligated to the manganese ion that undergoes oxidation during the $S_1$ to $S_2$ transition: an isotope-edited FTIR study. Biochemistry 43:3152–3166

Colthup NB, Daly LH, Wiberly SE (1975) Introduction to infrared and Raman spectroscopy. Academic Press, New York

Deacon GB, Phillips RJ (1980) Relationships between the carbon-oxygen stretching frequencies of carboxylato complexes and the type of carboxylate coordination. Coord Chem Rev 33:227–250

Debus RJ (2008) Protein ligation of the photosynthetic oxygen-evolving center. Coord Chem Rev 252:244–258

Deng H, Callender R (1999) Raman spectroscopic studies of the structures, energetics, and bond distortions of substrates bound to enzymes. Methods Enzymol 308:176–201

Di Donato M, Cohen RO, Diner BA, Breton J, van Grondelle R, Groot ML (2008) Primary charge separation in the photosystem II core from Synechocystis: a comparison of femtosecond visible/midinfrared pump-probe spectra of wild-type and two P680 mutants. Biophys J 94:4783–4795

Dupeyrat F, Vidaud C, Lorphelin A, Berthomieu C (2004) Long distance charge redistribution upon Cu, Zn-superoxide dismutase reduction—significance of dismutase function. J Biol Chem 279:48091–48101

Faller P, Debus RJ, Brettel K, Sugiura M, Rutherford AW, Boussac A (2001) Rapid formation of the stable tyrosyl radical in photosystem II. Proc Natl Acad Sci USA 98:14368–14373

Gourion-Arsiquaud S, Chevance S, Bouyer P, Garnier L, Montillet JL, Bondon A, Berthomieu C (2005) Identification of a $Cd^{2+}$ and $Zn^{2+}$ binding site in cytochrome c using FTIR coupled to an ATR micro-dialysis set-up and NMR spectroscopy. Biochemistry 44:8652–8663

Griffith PR, de Haseth JA (1986) Fourier transform infrared spectroscopy. Wiley, New York

Hasegawa K, Ono T, Noguchi T (2000) Vibrational spectra and ab initio DFT calculations of 4-methylimidazole and its different protonation forms: infrared and Raman markers of the protonation state of a histidine side chain. J Phys Chem B 104:4253–4265

Hasegawa K, Ono T, Noguchi T (2002) Ab initio DFT calculations and vibrational analysis of zinc-bound 4-methylimidazole as a model of a histidine ligand in metalloenzymes. J Phys Chem A 106:3377–3390

Hastings G, Ramesh VM, Wang R, Sivakumar V, Webber A (2001) Primary donor photo-oxidation in photosystem I: a re-evaluation of (P700(+) - P700) Fourier transform infrared difference spectra. Biochemistry 40:12943–12949

Hauser K, Krejtschi C, Huang R, Wu L, Keiderling TA (2008) Site-specific relaxation kinetics of a tryptophan zipper hairpin peptide using temperature-jump IR spectroscopy and isotopic labeling. J Am Chem Soc 130:2984–2992

Hienerwadel R, Berthomieu C (1995) Bicarbonate binding to the non-heme iron of photosystem II investigated by Fourier transform infrared difference spectroscopy and $^{13}$C-labeled bicarbonate. Biochemistry 34:16288–16297

Hienerwadel R, Thibodeau D, Lenz F, Nabedryk E, Breton J, Kreutz W, Mäntele W (1990) Time-resolved infrared spectroscopy of electron transfer in bacterial photosynthetic reaction centers: dynamics of binding and interaction upon QA and QB reduction. Biochemistry 31:5799–5808

Hienerwadel R, Grzybek S, Fogel C, Kreutz W, Okamura MY, Paddock ML, Breton J, Nabedryk E, Mäntele W (1995) Protonation of Glu L212 following $Q_B^-$ formation in the photosynthetic reaction center of *Rhodobacter sphaeroides*: evidence from time-resolved infrared spectroscopy. Biochemistry 34:2832–2843

Hienerwadel R, Boussac A, Breton J, Berthomieu C (1996) Fourier transform infrared difference study of tyrosineD oxidation and plastoquinone QA reduction in photosystem II. Biochemistry 35:15447–15460

Hienerwadel R, Boussac A, Breton J, Diner BA, Berthomieu C (1997) Fourier transform infrared difference spectroscopy of photosystem II tyrosine D using site-directed mutagenesis and specific isotope labeling. Biochemistry 36:14712–14723

Hienerwadel R, Diner BA, Berthomieu C (2008) Molecular origin of the pH dependence of tyrosine D oxidation kinetics and radical stability in photosystem II. Biochim Biophys Acta 1777:525–531

Iwaki M, Andrianambinintsoa S, Rich P, Breton J (2002) Attenuated total reflection Fourier transform infrared spectroscopy of redox transitions in photosynthetic reaction centers: comparison of perfusion- and light-induced difference spectra. Spectrochim Acta A Mol Biomol Spectrosc 58:1523–1533

Kandori H (2000) Role of internal water molecules in bacteriorhodopsin. Biochim Biophys Acta 1460:177–191

Karyakin A, Motiejunas D, Wade RC, Jung C (2007) FTIR studies of the redox partner interaction in cytochrome P450: the Pdx-P450cam couple. Biochim Biophys Acta 1770:420–431

Kimura Y, Mizusawa N, Ishii A, Ono T (2005) FTIR detection of structural changes in a histidine ligand during S-State cycling of photosynthetic oxygen-evolving complex. Biochemistry 44:16072–16078

Kötting C, Gerwert K (2005) Proteins in action monitored by time-resolved FTIR spectroscopy. ChemPhysChem 6:881–888

Krimm S, Bandekar J (1986) Vibrational spectroscopy and conformation of peptides, polypeptides, and proteins. Adv Prot Chem 38:181–364

Lehmann N, Aradhyam GK, Fahmy K (2002) Suramin affects coupling of rhodopsin to transducin. Biophys J 82:793–802

Leonhard M, Mäntele W (1993) Fourier transform infrared spectroscopy and electrochemistry of the primary electron donor in *Rhodobacter sphaeroides* and *Rhodopseudomonas viridis* reaction centers: vibrational modes of the pigments in situ and evidence for protein and water modes affected by P+ formation. Biochemistry 32:4532–4538

Levin IW, Bhargava R (2005) Fourier transform infrared vibrational spectroscopic imaging: integrating microscopy and molecular recognition. Ann Rev Phys Chem 56:429–474

Lorenz-Fonfria VA, Furutani Y, Kandori H (2008) Active internal waters in the bacteriorhodopsin photocycle. A comparative study of the L and M intermediates at room and cryogenic temperatures by infrared spectroscopy. Biochemistry 47:4071–4081

Mäntele W, Wollenweber AM, Nabedryk E, Breton J (1988a) Infrared spectroelectrochemistry of bacteriochlorophylls and bacteriopheophytins: implications for the binding of the pigments in the reaction center from photosynthetic bacteria. Proc Natl Acad Sci USA 85:8468–8472

Mäntele W, Wollenweber AM, Rashwan F, Heinze J, Nabedryk E, Berger G, Breton J (1988b) Fourier transform infrared spectroelectrochemistry of the bacteriochlorophyll a anion radical. Photochem Photobiol 47:451–456

Mayer G, Heckel A (2006) Biologically active molecules with a "light switch". Angew Chem 45:4900–4921

Mezzetti A, Seo D, Leibl W, Sakurai H, Breton J (2003) Time-resolved step-scan FTIR investigation on the primary donor of the reaction center from the green sulfur bacterium *Chlorobium tepidum*. Photosynth Res 75:161–169

Moss D, Nabedryk E, Breton J, Mäntele W (1990) Redox-linked conformational changes in proteins detected by a combination of infrared spectroscopy and protein electrochemistry. Evaluation of the technique with cytochrome c. Eur J Biochem 187:565–572

Mukherjee S, Chowdhury P, Bunagan MR, Gai F (2008) Folding kinetics of a naturally occurring helical peptide: implication of the folding speed limit of helical proteins. J Phys Chem B 112: 9146–9150

Nabedryk E (1996) Light-induced Fourier transform infrared difference spectroscopy of the primary electron donor in photosynthetic reaction centers. In: Mantsch HH, Chapman D (eds) Infrared spectroscopy of biomolecules. Wiley-Liss, New York, pp 39–81

Nabedryk E, Breton J (2008) Coupling of electron transfer to proton uptake at the QB site of the bacterial reaction center: a perspective from FTIR difference spectroscopy. Biochim Biophys Acta 1777:1229–1248

Nabedryk E, Leonhardt M, Mäntele W, Breton J (1990a) Fourier transform infrared difference spectroscopy shows no evidence for an enolization of chlorophyll a upon cation formation either in vitro or during P700 photooxidation. Biochemistry 29:3242–3247

Nabedryk E, Bagley KA, Thibodeau DL, Bauscher M, Mäntele W, Breton J (1990b) A protein conformational change associated with the photoreduction of the primary and secondary quinones in the bacterial reaction center. FEBS Lett 266:59–62

Nabedryk E, Breton J, Hienerwadel R, Fogel C, Mäntele W, Paddock ML, Okamura MY (1995) Fourier transforms infrared difference spectroscopy of secondary quinone acceptor photoreduction in proton transfer mutants of *Rhodobacter sphaeroides*. Biochemistry 34:14722–14732

Nakamoto K (1997) Infrared and Raman spectra of inorganic and coordination compounds. Part b, 5th edn. Wiley, New York, pp 59–62

Nie B, Stutzman J, Xie A (2005) A vibrational spectral marker for probing the hydrogen-bonding status of protonated Asp and Glu residues. Biophysical J 88:2833–2847

Noguchi T (2007) Light-induced FTIR difference spectroscopy as a powerful tool toward understanding the molecular mechanism of photosynthetic oxygen evolution. Photosynth Res 91:59–69

Noguchi T (2008) Fourier transform infrared analysis of the photosynthetic oxygen-evolving center. Coord Chem Rev 252: 336–346

Noguchi T, Berthomieu C (2005) Molecular analysis by vibrational spectroscopy. In: Wydrzynski T, Satoh K (eds) Photosystem II: the light-drivenwater/plastoquinone oxidoreductase, vol 16. Springer, Dordrecht, The Netherlands, pp 367–387

Noguchi T, Sugiura M (2000) Structure of an active water molecule in the water-oxidising complex of photosystem II as studied by FTIR spectroscopy. Biochemistry 39:10943–10949

Noguchi T, Sugiura M (2002a) Flash-induced FTIR difference spectroscopy of the water oxidizing complex in moderately hydrated photosystem II core films: effect of hydration extent on S-state transitions. Biochemistry 41:2322–2330

Noguchi T, Sugiura M (2002b) FTIR detection of water reactions during the flash-induced S-state cycle of the photosynthetic water-oxidizing complex. Biochemistry 41:15706–15712

Noguchi T, Sugiura M (2003) Analysis of flash-induced FTIR difference spectra of the S-state cycle in the photosynthetic water-oxidizing complex by uniform $^{15}N$ and $^{13}C$ isotope labeling. Biochemistry 42:6035–6042

Noguchi T, Mitsuka T, Inoue Y (1994) Fourier transform infrared spectrum of the radical cation of beta-carotene photoinduced in photosystem II. FEBS Lett 356:179–182

Noguchi T, Ono T, Inoue Y (1995) Direct detection of a carboxylate bridge between Mn and $Ca^{2+}$ in the photosynthetic oxygen-evolving center by means of Fourier transform infrared spectroscopy. Biochim Biophys Acta 1228:189–200

Noguchi T, Inoue Y, Tang X-S (1997) Structural coupling between the oxygen-evolving Mn cluster and a tyrosine residue in photosystem II as revealed by Fourier transform infrared spectroscopy. Biochemistry 36:14705–14711

Noguchi T, Tomo T, Inoue Y (1998) Fourier transform infrared study of the cation radical of P680 in the photosystem II reaction center: evidence for charge delocalization on the chlorophyll dimer. Biochemistry 37:13614–13625

Noguchi T, Inoue Y, Tang X-S (1999) Structure of a histidine ligand in the photosynthetic oxygen-evolving complex as studied by light-induced Fourier transform infrared difference spectroscopy. Biochemistry 38:10187–10195

O'Malley PJ (2002) Density functional calculations modeling tyrosine oxidation in oxygenic photosynthetic electron transfer. Biochim Biophys Acta 1553:212–217

Pantelidou M, Chitnis PR, Breton J (2004) FTIR spectroscopy of *Synechocystis* 6803 mutants affected on the hydrogen bonds to the carbonyl groups of the PsaA chlorophyll of P700 supports an extensive delocalization of the charge in $P_{700}{}^{+}$. Biochemistry 43:8380–8390

Petibois C, Déléris G (2006) Chemical mapping of tumor progression by FT-IR imaging: towards molecular histopathology. Trends Biotechnol 24:455–462

Rich P, Iwaki M (2007) Methods to probe protein transitions with ATR infrared spectroscopy. Mol BioSyst 3:398–407

Rose S, Minagawa J, Seufferheld M, Padden S, Svensson B, Kolling DRJ, Crofts AR, Govindjee (2008) D1-arginine mutants (R257E, K and Q) of *Chlamydomonas reinhardtii* have a lowered QB

redox potential: analysis of thermoluminescence and fluorescence measurements. Photosynth Res 98:449–468

Rothschild K, Zagaeski M, Cantore WA (1981) Conformational changes of bacteriorhodopsin detected by Fourier transform infrared difference spectroscopy. Biochem Biophys Res Comm 103:483–489

Siebert F, Hildebrandt P (2008) Vibrational spectroscopy in life science. Wiley-VCH Verlag GmbH & Co. KGaA, Weinheim, Germany

Sivakumar V, Wang R, Hastings G (2005) $A_1$ reduction in intact cyanobacterial photosystem I particles studied by time-resolved step-scan Fourier transform infrared difference spectroscopy and isotope labeling. Biochemistry 44:1880–1893

Socrates G (1994) Infrared characteristic group frequencies: tables and charts, 2nd edn. Wiley, Chichester

Strickler MA, Hillier W, Debus J (2006) No evidence from FTIR difference spectroscopy that glutamate-189 of the D1 polypeptide ligates a Mn ion that undergoes oxidation during the $S_0$ to $S_1$, $S_1$ to $S_2$, or $S_2$ to $S_3$ transitions in photosystem II. Biochemistry 45:8801–8811

Strickler MA, Walker LM, Hillier W, Britt RD, Debus J (2007) No evidence from FTIR difference spectroscopy that aspartate-342 of the D1 polypeptide ligates a Mn ion that undergoes oxidation during the $S_0$ to $S_1$, $S_1$ to $S_2$, or $S_2$ to $S_3$ transitions in photosystem II. Biochemistry 46:3151–3160

Takahashi R, Noguchi T (2007) Criteria for determining the hydrogen-bond structures of a tyrosine side chain by Fourier transform infrared spectroscopy: density functional theory analyses of model hydrogen-bonded complexes of p-cresol. J Phys Chem B 111: 13833–13844

Takahashi R, Sugiura M, Noguchi T (2007) Water molecules coupled to the redox-active tyrosine YD in photosystem II as detected by FTIR spectroscopy. Biochemistry 46:14245–14249

Thibodeau DL, Nabedryk E, Hienerwadel R, Lenz F, Mäntele W, Breton J (1990) Time-resolved FTIR spectroscopy of quinones in the *Rb. sphaeroides* reaction centers. Biochim Biophys Acta 1020:253–259

Van Rensen JJS, Xu C, Govindjee (1999) Role of bicarbonate in the photosystem II, the water-plastoquinone oxido-reductase of plant photosynthesis. Physiol Plant 105:585–592

Venyaminov SY, Kalnin NN (1990a) Quantitative IR spectrophotometry of peptide compounds in water ($H_2O$) solutions. I. Spectral parameters of amino acid residue absorption bands. Biopolymers 30:1243–1257

Venyaminov SY, Kalnin NN (1990b) Quantitative IR spectrophotometry of peptide compounds in water ($H_2O$) solutions. II. Amide absorption bands of polypeptides and fibrous proteins in alpha, beta-, and random coil conformations. Biopolymers 30:1259–1271

Vidaud C, Gourion-Arsiquaud S, Rollin-Genetet F, Albert C, Plantevin S, Pibbe O, Berthomieu C, Quemeneur E (2007) Structural consequences of $UO_2^{2+}$ binding to apotransferrin: can this protein account for uranium entry into human cells? Biochemistry 46: 2215–2226

Weidlich O, Siebert F (1993) Time-resolved step-scan FT-IR investigations of the transition from KL to L in the bacteriorhodopsin photocycle: identification of chromophore twists by assigning hydrogen-out-of-plane (HOOP) bending vibrations. Appl Spectrosc 47:1394–1400

Wolpert M, Hellwig P (2006) Infrared spectra and molar absorption coefficients of the 20 alpha amino acids in aqueous solutions in the spectral range from 1800 to 500 $cm^{-1}$. Spectrochim Acta A 64: 987–1001

Wydrzynski TJ, Satoh S (2005) Photosystem II—the light-driven water: plastoquinone oxidoreductase. Advances in photosynthesis and respiration, vol 22. Springer, Dordrecht

Yamanari T, Kimura Y, Mizusawa N, Ishii A, Ono T (2004) Mid to low-frequency Fourier transform infrared spectra of S-state cycle for photosynthetic water oxidation in *Synechocystis* sp PCC 6803. Biochemistry 43:7479–7490

Yamazaki Y, Hatanaka M, Kandori H, Sasaki J, Karstens WF, Raap J, Lugtemburg J, Bizounok M, Herzfeld J, Needleman R, Lanyi JK, Maeda A (1995) Water structural changes at the proton uptake site (the Thr46-Asp96 domain) in the L intermediate of bacteriorhodopsin. Biochemistry 34:7088–7093